



## Layer silicates modified with 1,4-bis(3-aminopropyl)piperazine for the removal of Th(IV), U(VI) and Eu(III) from aqueous media

Denis L. Guerra<sup>a,\*</sup>, Alane A. Pinto<sup>a</sup>, Rúbia R. Viana<sup>b</sup>, Claudio Airoidi<sup>a</sup>

<sup>a</sup> Chemistry Institute, State University of Campinas, P.O. Box 6154, 13084-971 Campinas, São Paulo, Brazil

<sup>b</sup> Universidade Federal de Mato Grosso, UFMT, Centro de Recursos Minerais, Cuiabá, Mato Grosso 78060 900, Brazil

### ARTICLE INFO

#### Article history:

Received 1 March 2009

Received in revised form 24 May 2009

Accepted 1 June 2009

Available online 17 June 2009

#### Keywords:

Montmorillonite

Kanemite

Radionuclide

Adsorption

Thermodynamic

### ABSTRACT

Natural montmorillonite (M) and synthetic kanemite (K) have been functionalized with 1,4-bis(3-aminopropyl)piperazine reacted with methylacrylate to yield new inorganic–organic chelating materials. The original and modified materials were characterized by X-ray diffractometry, textural analysis, SEM and nuclear magnetic nuclei of carbon-13 and silicon-29. The chemically modified clay samples (M-APPMA and K-APPMA) showed modification of their physical–chemical properties including: specific area  $45.0 \text{ m}^2 \text{ g}^{-1}$  (M) to  $978.8 \text{ m}^2 \text{ g}^{-1}$  (M-APPMA) and  $275 \text{ m}^2 \text{ g}^{-1}$  (K) to  $898.9 \text{ m}^2 \text{ g}^{-1}$  (K-APPMA). The ability of these materials to remove thorium(IV), uranyl(VI) and europium(III) from aqueous solution was followed by a series of adsorption isotherms, which were fitted to non-linear Sips adsorption isotherm model. To achieve the best adsorption conditions the influence of pH and variation of metal concentration were investigated. The energetic effects ( $\Delta_{\text{int}}H^\circ$ ,  $\Delta_{\text{int}}G^\circ$  and  $\Delta_{\text{int}}S^\circ$ ) caused by metal ions adsorption were determined through calorimetric titrations.

© 2009 Published by Elsevier B.V.

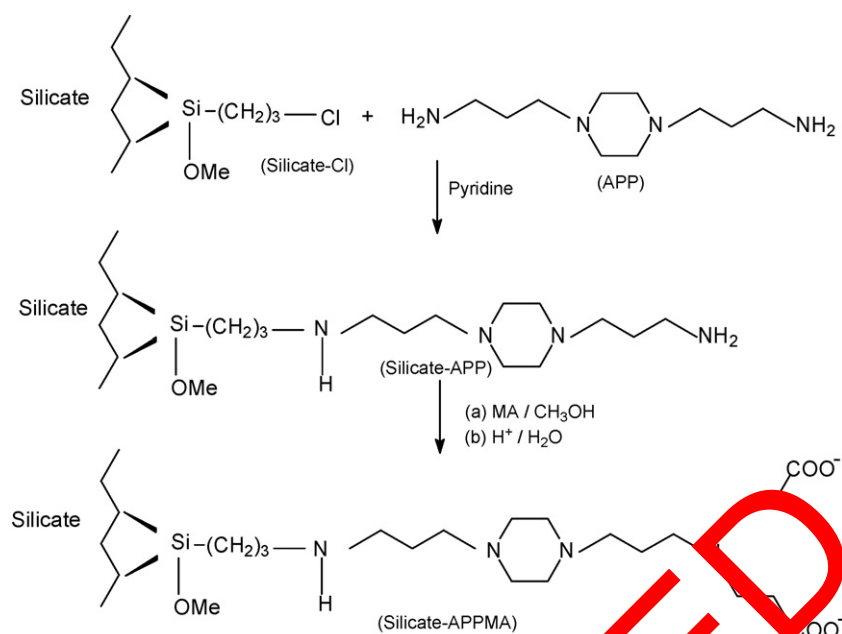
### 1. Introduction

Environmental concerns associated with disposal of toxic metal ions such as Th(IV), U(VI) and Eu(III) in natural waters and wastes have encouraged the development of new materials with the ability to remove this kind of contaminant from solvents. The preparation of modified phyllosilicates and zeolites with groups that present chemical affinity with these contaminants is one of the proposed solutions for these environmental problems [1,2]. Since heavy metals have toxic effects on the environment and human life, the removal of heavy metal ions from polluted waters is currently one of the more important environmental challenges [3–5]. When toxic metals are present in the aquatic system, the abatement of the pollutant to an acceptable level is necessary. The toxic nature of these radionuclides, even at trace levels, has been a public health problem for many years, the exposure of these elements to plants and human being occurs through ingestion of foodstuffs and by drinking water. After accumulating, these toxic elements clearly interface in the physiological systems of living organisms [6]. Thus, the synthesis of new adsorbents having desirable properties for toxic/heavy metal ions removal from aqueous systems is a subject of continuing research interest with a view to control pollution in the environment [7].

Solid acids and bases have been used to remove contaminants dispersed in solvents, and the development of solid bases and acids to be used with solid catalyst instead of a liquid is becoming common [8,9]. Moreover, the use of solid bases and acids to remove contaminants has the great advantage of allowing a larger number of processing options such as fluidized and fixed bed reactors [10]. The advances in layer material organofunctionalization field are closely associated with development of new silylating agents, which pendant organic chains can display non-hydrolysable silicon–carbon bond, to prevent the leaching of the immobilized reagent to solution. However, as the pendant chains incorporate donor basic reactive atoms, an improvement on adsorption and exchange properties are generally increased [11]. For this purpose, the enlargement in organic chains through successive reactions, by including functional groups give well-defined conditions in determining ultimate properties, such as applications in various technological processes [11].

Adsorption is a simple and robust procedure with high efficiency for industrial treatment of effluents. Inorganic–organic materials are the most employed adsorbent for heavy metal removal from aqueous solution [12]. However, the extensive use of hybrids materials for metal removal from industrial effluents is expensive, limiting its large application for wastewater treatment [13]. The potential activity of such hybrid materials in binding metal ions can be explained by the complexation chemistry principles, by involving ligand–metal interaction, which depends on the specificity of a particular ligand toward target metal ions, the result being a conventional acid–base bonding between them. Although

\* Corresponding author. Tel.: +55 19 33429407; fax: +55 19 33429407.  
E-mail address: [diguerra@iqm.unicamp.br](mailto:diguerra@iqm.unicamp.br) (D.L. Guerra).



**Scheme 1.** Sequence of reactions for immobilization.

some amino-functionalized adsorbents can exhibit specific interactions with hard Lewis acids, the selectivity of these materials is usually unremarkable, because many metals have great ability to bind amine ligands [14].

The present investigation reports the functionalization of phyllosilicates with 1,4-bis(3-aminopropyl)piperazine and subsequent reaction with methylacrylate in heterogeneous route, to yield final products containing carboxylate moieties in the structures, with a further potential to grow using a divergent synthetic approach. The unmodified and modified matrices were used as adsorbents to extract  $\text{Th}^{4+}$ ,  $\text{UO}_2^{2+}$  and  $\text{Eu}^{3+}$  from aqueous solutions at room temperature and pH 4.0. The present methodology opens a new initiative for clays having immobilized supramolecular chemistry and the characterized materials were explored for thorium(IV), uranyl(VI) and europium(III) adsorption properties.

## 2. Materials and methods

### 2.1. Preparation of functionalized clay samples

The montmorillonite was sampled in the Amazon region, in northern Brazil. Size fractions of less than  $2\ \mu\text{m}$  were separated by sedimentation. The cation-exchange capacity (CEC) was determined by the ammonium acetate method with concentrations of  $2.0\ \text{mol dm}^{-3}$  at pH 8.0.

The Na-kanemite ( $\delta\text{-Na}_2\text{Si}_2\text{O}_5$ ) was prepared by reaction of  $\text{SiO}_2$  and  $\text{Na}_2\text{O}$  ( $\text{SiO}_2/\text{Na}_2\text{O}=2$ ) in  $500.0\ \text{cm}^3$  of ethanol. The  $20.0\ \text{g}$  of sodium silicate gel were calcinated at  $973 \pm 1\ \text{K}$  for 6 h to obtained  $\delta\text{-Na}_2\text{Si}_2\text{O}_5$ . After calcination, the resulting solid was stirred by 3 h at  $77 \pm 1\ \text{K}$  in nitrogen atmosphere. Centrifugation of the dispersion gave us a Na-kanemite paste [15]. The resulting material was dried in  $318 \pm 1\ \text{K}$  and named K.

A heterogeneous route was adopted to chemically inorganic structure of silicates with functional groups. A divergent synthetic approach was made for the preparation of amine-terminated wedge, and a subsequent carboxylate terminated wedge in the structure, as shown in Scheme 1.

In the first step, a sample of  $15.0\ \text{g}$  of each silicate was activated by refluxing with concentrated HCl for 4.5 h to remove any adsorbent metal ions, then filtrated and repeatedly washed with

water until the filtrate of each sample was neutral and dried in an oven at  $370 \pm 1\ \text{K}$  for 9 h to remove adsorbed surface water. Further, it was heated in a stream of dry nitrogen at  $77 \pm 1\ \text{K}$  for 3 h and was immediately used. The organochloro functional agent was then immobilized by suspending samples of  $14.0\ \text{g}$  of dry activated silicate in  $50.0\ \text{cm}^3$  of dry xylene, followed by addition of  $4.5\ \text{cm}^3$  of 3-chloropropyltrimethoxysilane to the suspensions. The mixtures were allowed to react under continuous stirring and a dry nitrogen atmosphere at  $340 \pm 1\ \text{K}$  for 80 h. The suspensions were filtered, washed with xylene, methanol and dried under vacuum [16], the resulting products were called M-Cl and K-Cl (silicate-Cl). In the subsequent step the suspensions of  $12.0\ \text{g}$  of M-Cl and K-Cl in  $50.0\ \text{cm}^3$  of xylene were allowed to react with  $15.0\ \text{cm}^3$  of 1,4-bis(3-aminopropyl)piperazine (APP) at  $340 \pm 1\ \text{K}$  under continuous stirring and a dry nitrogen atmosphere for 48 h. The resulting solids, M-APP and K-APP (silicate-APP) were filtered, washed with xylene and an excess of ethanol and then dried under vacuum. In the subsequent step, samples of  $10\ \text{g}$  of each silicate-APP reacted with  $10.0\ \text{cm}^3$  of methylacrylate (MA) in  $70.0\ \text{cm}^3$  of methanol at a controlled temperature of  $325 \pm 1\ \text{K}$  and under a nitrogen atmosphere for 50 h to yield the final products, named M-APPMA and K-APPMA (silicate-APPMA). The resulting solids were washed with an excess of methanol, dried, and then treated with  $50.0\ \text{cm}^3$  of diluted hydrochloric acid ( $0.1\ \text{mol dm}^{-3}$ ) for 2 h, and then again washed with methanol and further dried under vacuum.

### 2.2. Characterization of phyllosilicates

X-ray powder diffraction (XRD) patterns were recorded with a Philips PW 1050 diffractometer using  $\text{Cu K}\alpha$  ( $0.154\ \text{nm}$ ) radiation in the region between  $2^\circ$  and  $65^\circ$  ( $2\theta$ ) at a speed of  $2^\circ/\text{min}$  and a step of  $0.050^\circ$ .

The silicate samples were analyzed by scanning electron microscopy (SEM) images were recorded on a model LEO-ZEISS, 430 Vp, in conditions of analysis using secondary images using an acceleration voltage of  $20\ \text{kV}$  and magnification ranging from 100 to 20,000-fold.

Brunauer-Emmett-Teller (BET) surface area [17], pore diameter and pore volume were obtained from nitrogen adsorption/desorption in a Micromeritics ASAP 2000 BET surface analyzer

system. The mesopore size distribution was obtained by applying the Barret–Joyner–Halenda (BJH) method to the adsorption branch of the isotherm [18].

Nuclear magnetic resonance spectra in the solid-state were recorded from Bruker AC 300/P spectrometer at room temperature. For each spectrum about 1 g of each solid sample was compacted into a 7 mm zirconium oxide rotor. The measurements were obtained at frequencies of 59.63 and 75.47 MHz, for silicon and carbon, respectively, with a magic-angle spinning of 4 kHz. In order to increase the signal-to-noise ratio of the solid-state spectra, the technique of magic-angle spinning NMR (MAS-NMR) was used, with pulse repetitions of 3 s and contact time of 1 ms [19].

Elemental analysis (%N and %C) was done on a PerkinElmer, model 2400, elemental analyzer.

### 2.3. Adsorption and thermodynamic

The adsorption experiments were performed through the batch-wise method by suspending a series of 20 mg samples of the each phyllosilicate, in 20.0 cm<sup>3</sup> aqueous solutions of cations at concentrations varying from 1.25 to 2.50 × 10<sup>-2</sup> mmol dm<sup>-3</sup>, under orbital stirring for 24 h at 298 ± 1 K. Profiles of the obtained adsorption isotherms represented by the number of moles adsorbed (*N<sub>f</sub>*) versus the number of moles at equilibrium per volume of solution (*C<sub>s</sub>*), for series of isotherms, the data reveals that the adsorption process conforms to the Sips model. Sips combined the Langmuir and Freundlich equations (Eq. (1)) [20]. The Sips isotherm is a three parameter fitting equation and combines the features of both Freundlich and Langmuir models. The Freundlich–Langmuir isotherm model (Sips) is the combination of Freundlich isotherm and Langmuir isotherm model. It will give a Langmuir isotherm model when *n* is equal to 1 (Eq. (1)):

$$N_f = \frac{N_s K_S C_s^{1/n}}{1 + K_S C_s^{1/n}} \quad (1)$$

where *C<sub>s</sub>* is the concentration of solution at equilibrium (mol dm<sup>-3</sup>), *N<sub>f</sub>* and *N<sub>s</sub>* are the concentration of radionuclides adsorbed and the maximum amount of radionuclides adsorbed per gram of material (mol g<sup>-1</sup>), respectively, which depend on the number of available adsorption reactive sites, *K<sub>S</sub>* is the equilibrium constant and *n* is the Freundlich exponent [20].

The thermal effects from metal cation interacting on modified clay samples were followed by calorimetric titration using an isothermal calorimeter, Model LK 2277, from Thermometric. In this titration, the metallic solution was added to a suspension of about 20 mg of clay sample in 2.0 cm<sup>3</sup> of water, under stirring at 298 ± 1 K. A series of increments of 10 μL of metal solutions was added to the metals–clay to obtain the thermal effect interaction (*Q<sub>tit</sub>*). Two other titrations are needed to complete the full experiment: (i) the thermal effect due to hydration of the clays (*Q<sub>hid</sub>*), which normally gives a null value and (ii) the dilution effect of metal solutions in water, without sample in the vessel (*Q<sub>dil</sub>*). The integrated heat value is obtained by use of the data treatment Digitam 4.1 program (Thermometric). The resulting thermal effect is given by the following Eq. (2) [21]:

$$\sum Q_r = \sum Q_{tit} - \sum Q_{dil} \quad (2)$$

The molar enthalpy ( $\Delta H^\circ$ ) of the process can be calculated by Eq. (2).

$$\Delta_{int}H^\circ = \Delta_{int}h^\circ N_s \quad (3)$$

The Gibbs free energy can be calculated by Eq. (4), the entropy is finally calculated from Eq. (5) [22–24]. The pH of the solutions was

measured using pH/Ion Analyzer, model 450 M.

$$\Delta_{int}G^\circ = -RT \ln K_S \quad (4)$$

$$\Delta_{int}G^\circ = \Delta_{int}H^\circ - T\Delta_{int}S^\circ \quad (5)$$

The thoriumnitrate [Th(NO<sub>3</sub>)<sub>4</sub>·5H<sub>2</sub>O, CDH, 99.99%], europium(III) oxide (Eu<sub>2</sub>O<sub>3</sub>, Himedia, 99.99%) and uranylacetate [UO<sub>2</sub>(CH<sub>3</sub>COO)<sub>2</sub>·2H<sub>2</sub>O, BDH, 99.99%] were used as a source of Th(IV), Eu(III) and U(VI), respectively. A simple and sensitive spectrophotometric method based on colored complexes, Arsenazo III [2,7-bis (2-arsenophenylazo)chromotropic acid, C<sub>22</sub>H<sub>18</sub>As<sub>2</sub>N<sub>4</sub>Na<sub>2</sub>O<sub>14</sub>S<sub>2</sub>·4H<sub>2</sub>O, Merck, 99.99%] with U(VI) and Th(IV) and Alizarin Red-S [sodium alizarinsulfonate, COC<sub>6</sub>H<sub>4</sub>COC<sub>6</sub>H(OH)<sub>2</sub>SO<sub>3</sub>NaH<sub>2</sub>O, CDH, 99.99%] with Eu(III) in aqueous medium was used for their determination. The concentrations of metal ions in the supernatant were determined with a Systronic-117 UV–vis spectrophotometer, by measuring absorbance at λ<sub>max</sub> of 660 nm for Th(IV), 652 nm for U(VI) and 531 nm for Eu(III) [25]. For each experimental point, the reproducibility was checked by at least one duplicate run.

## 3. Results and discussion

### 3.1. X-ray powder diffraction

X-ray powder diffraction of M, K, M-APPMA and K-APPMA showed significant changes. In Fig. 1a and b an increase in the interlayer distances of the original phyllosilicates is observed after the chemical modification process, by changing *d*<sub>001</sub> from 1.481 to 2.130 nm (M-APPMA) and 1.342 to 2.084 nm (K-APPMA) for the modified clays, in Fig. 1a and b, respectively. This is attributed to the presence of APPMA molecules that were intercalated in the crystal structure and the interaction of the intercalated species with reactive centers anchored in the surface of original phyllosilicates, such as the silanol groups [26]. The great influence of the number of APPMA ions on the surface and on the constitution and distribution of the ions has been previously reported [27]. The mass fraction of intercalation material can be estimated as the relative intensities of the reflection originating from the ‘unchanged’ and the ‘expanded’ layers. In the intercalated samples, the degree of reaction could be estimated as 81.05% (M-APPMA) and 75.01% (K-APPMA). This indicates that the APPMA molecules arrange in monolayer between the phyllosilicate layers [15].

### 3.2. <sup>29</sup>Si and <sup>13</sup>C NMR

Nuclear magnetic resonance in the solid-state is a technique to give valuable information about the bonding of the pendant chains anchored on an inorganic backbone. For this purpose carbon and silicon nuclei were examined in order to better characterize the synthetic compounds. For silicon, the spectra shown in Fig. 2a and b provide information about the polysiloxane framework such as various local environments of atoms involved and the attachment of pendant groups, and in the present case the assignments were based on a previously studied analogous system [11,27]. The modified silicate samples, M-APPMA and K-APPMA, showed for the silicon nucleus four main peaks located at –58.0, –68.0, –99.1 and –110.0 ppm. The first peak at –58.0 ppm was assigned to silicon atom of the silylating agent bonded to one OH group and forming two siloxane bonds with silicon atom of silicate structures, RSi(OSi)(OH)<sub>2</sub>, assigned as a T<sup>2</sup> signal. The peak at –68.0 ppm is attributed silicon atom in the RSi(OSi)<sub>3</sub> structure, with the signal named T<sup>4</sup>. The results indicated the covalent-attachment of organic groups on the montmorillonite and kanemite surfaces. The other two peaks, attributed to surface signals, are described as: (i) Si(OSi)<sub>4</sub>, Q<sup>4</sup> at

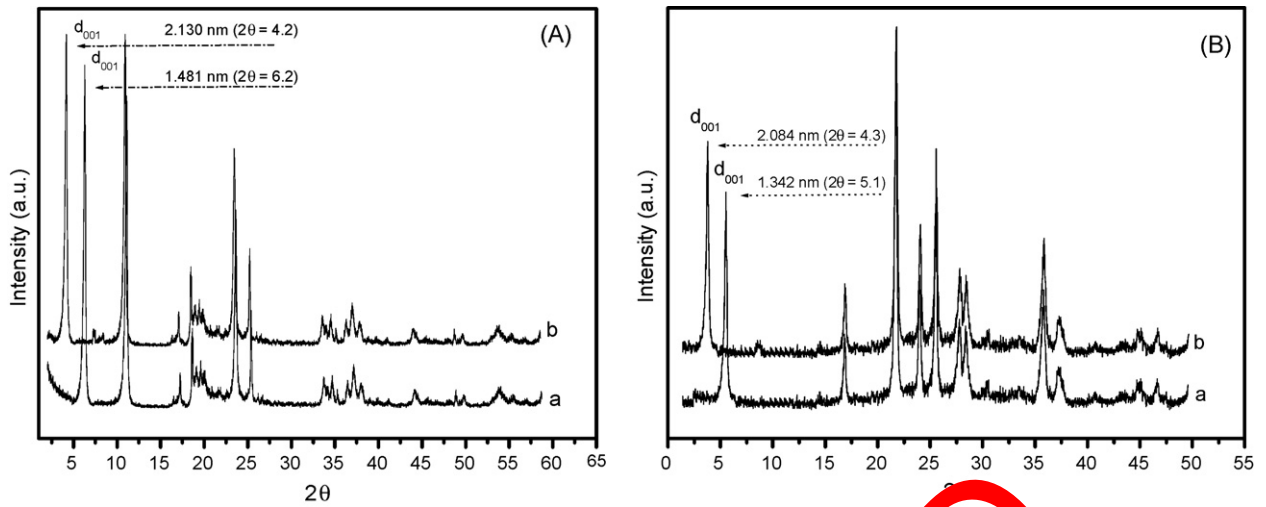


Fig. 1. X-ray diffraction patterns of original (a) and modified (b) clays: M and M-APPMA (A) and K and K-APPMA (B).

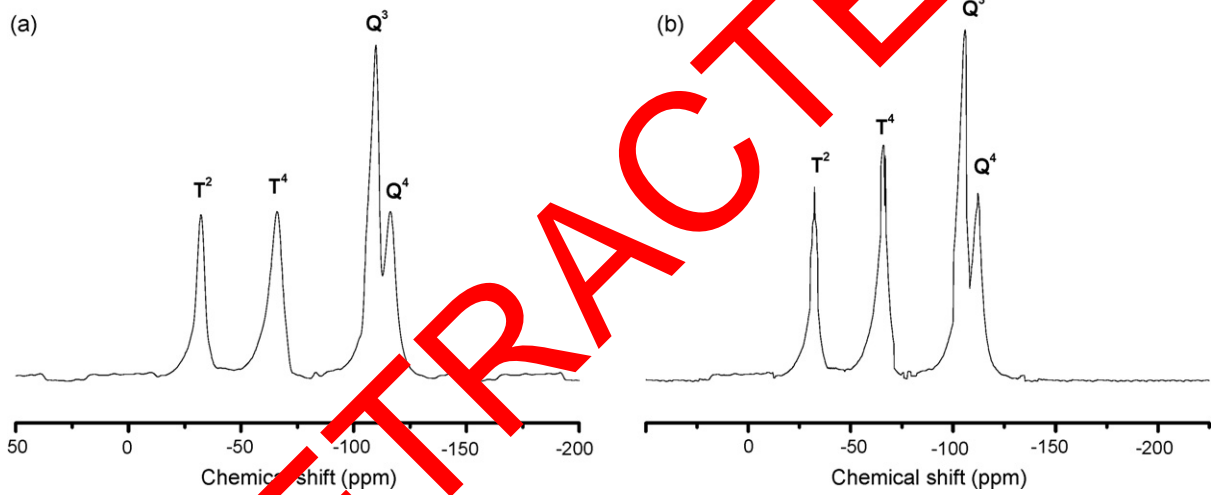


Fig. 2.  $^{29}\text{Si}$  NMR spectra of modified clays (M-APPMA) (a) and (K-APPMA) (b).

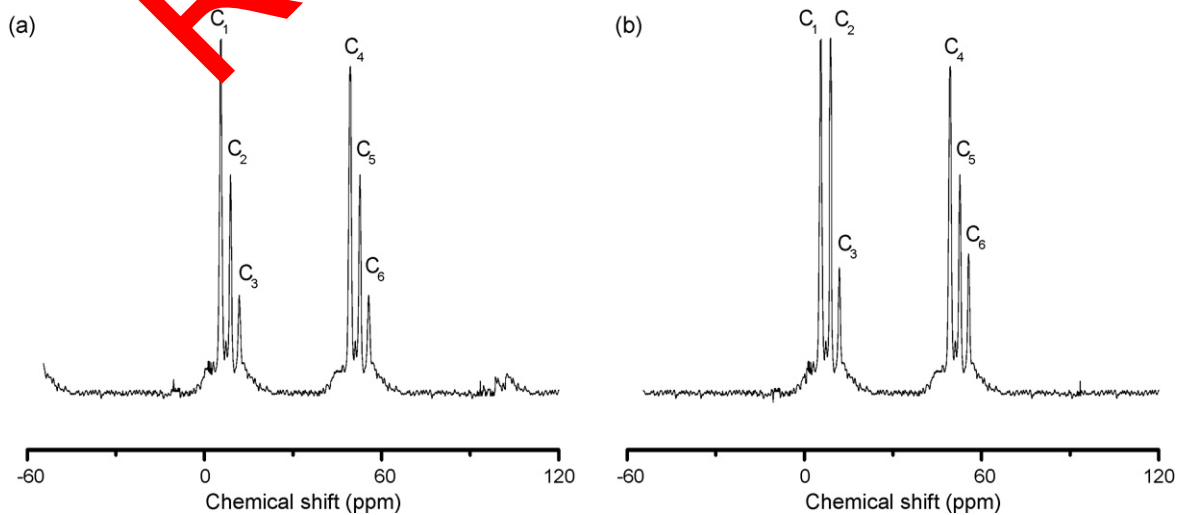


Fig. 3.  $^{13}\text{C}$  NMR spectra of modified clays (M-APPMA) (a) and (K-APPMA) (b).



**Table 1**  
Textural proprieties and quantification of organic molecules: original (M and K) and modified clay samples (M-APPMA and K-APPMA).

Sample	Surface area ( $SA_{BET}$ ) ( $m^2 g^{-1}$ )	Micropore area ( $m^2 g^{-1}$ )	Average pore diameter (nm)	Pore volume ( $cm^3 g^{-1}$ )	$d$ (molecules $nm^{-2}$ )	$l$ (nm)
K	23.5	0.9	1.2	0.08	–	–
M	45.0	10.0	2.3	0.09	–	–
K-APPMA	898.9	29.0	3.7	0.28	0.78	1.09
M-APPMA	978.8	37.1	4.7	0.30	0.83	1.11

–110.0 ppm and (ii) surface signal,  $Si(OSi)_3OH$ ,  $Q^3$  at –99.1 ppm [28].

The spectra related to  $^{13}C$  NMR in solid-state are shown in Fig. 3a and b for both modified silicates. These data correlate the important information regarding the immobilization of pendant chains on the inorganic backbone of natural montmorillonite and original kanemite structures. For two matrices the peaks at 10.5, 17.8 and 22.4 ppm were signed  $C_1$ ,  $C_2$  and  $C_3$  atoms of the aliphatic propyl chain of the immobilized organochloro compound. The peak centered at 51.1 ppm ( $C_4$ ) is assigned to the methylene group vibration in the compound. The peaks 54.0 ppm ( $C_5$ ) at 58.1 ppm ( $C_6$ ) denotes the carbon atoms from either unreacted alkoxy groups or structure anchored alkoxy groups [11,29].

The quantities of molecules attached to the modified clay surfaces,  $L_0 = 1.00 mmol g^{-1}$  (K-APPMA) and  $1.09 mmol g^{-1}$  (M-APPMA) were calculated from the percentage of nitrogen in the functionalized clay samples, as estimated by elemental analysis, using the following expression (Eq. (6)) [30,31]:

$$L_0 = \frac{\%N \times 10}{\text{nitrogen atomic weight}} \quad (6)$$

The C/N molar ratio calculated from the elemental analysis of M-APPMA and K-APPMA indicates a 1:2 stoichiometry, between the silanol groups on the clays surfaces and the silylating agent. Taking into account  $L_0$  and specific area ( $SA_{BET}$ ) of the modified

clays, the average surface density,  $d$ , of the attached molecules and average intermolecular distance,  $l$ , can be calculated by applying the following Eqs. (7) and (8) [30,31]:

$$d = N_A \frac{L_0}{SA_{BET}} \quad (7)$$

$$l = \left(\frac{1}{d}\right)^{1/2} \quad (8)$$

where  $N_A$  is Avogadro's number. The results obtained confirm a high efficiency in the chemical modification of the montmorillonite and kanemite samples. Thus, the high functionalization degree obtained in the modified clays can be explained by means of its modification of physical–chemical properties (Table 1).

### 3.3. Textural analysis and CEC of montmorillonite

The nitrogen adsorption values for original and modified phyllosilicates are listed in Table 1. The specific surface areas were calculated by the nitrogen BET method mainly for comparative purpose. The BET surface areas of the modified phyllosilicate samples demonstrated that chemical modification with caused the formation of micropores in the solid particles, resulting in a higher surface area, revealing 978.8 and 898.9  $m^2 g^{-1}$  for M-APPMA and K-APPMA, respectively. The pore size distribution in the mesopore region was obtained by applying the BJH method from nitrogen isotherms at

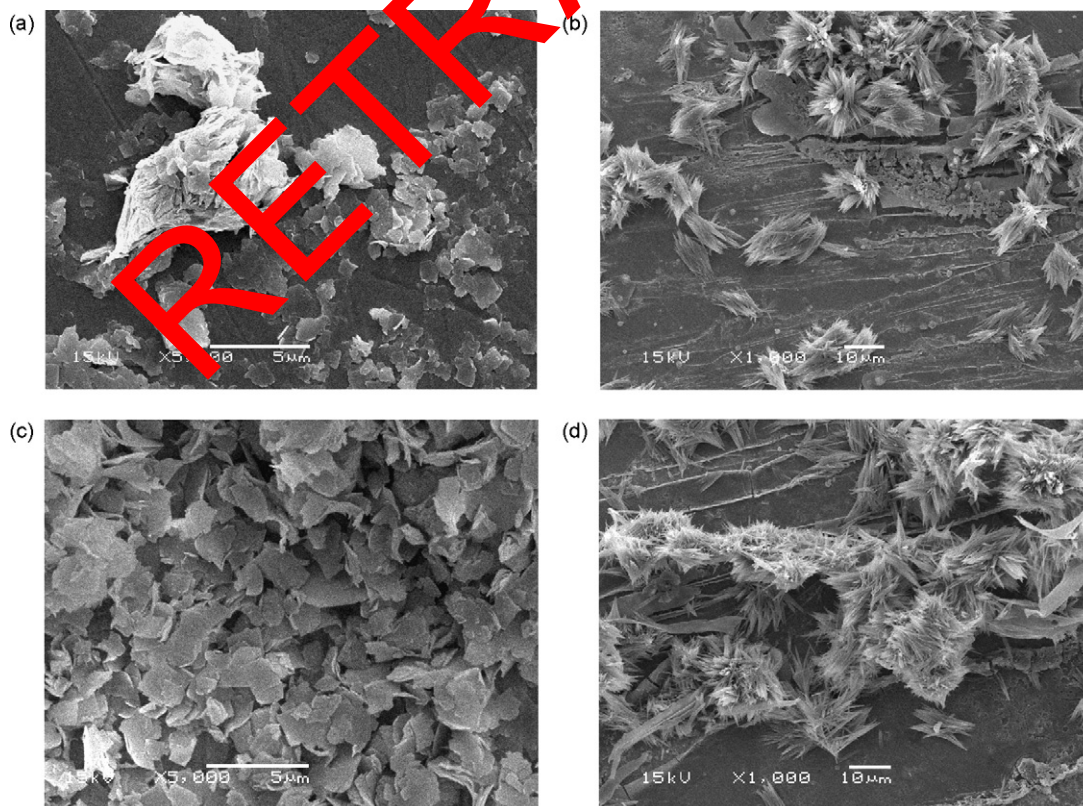


**Fig. 4.** SEM of original and modified clays: M (a), K (b), M-APPMA (c) and K-APPMA (d).

$77 \pm 1$  K. A change in pore size distribution was observed by comparing the original and modified clay samples. The samples have mostly mesopores, in which natural montmorillonite exhibited the maximum in differential pore volumes, to give 2.3 nm in pore diameter, while for modified phyllosilicates the pore diameters were 4.7 nm (M-APPMA) and 3.7 nm (K-APPMA). The modified phyllosilicates presented a unimodal distribution of pore size while M and K a bimodal distribution, in concordance with previous results [31]. The cation-exchange capacity (CEC) was measured in order to evaluate the potential use of clays for intercalation. The result obtained was 115.0 mequiv./100 g of clay (M) on an air-dried basis. The result obtained is in concordance with values obtained to mineral smectite groups (2:1) and other occurrences of montmorillonite in different sediment types, such as the montmorillonite sample (SWy-2-USA), the CEC was measured as 153.0 mequiv./100 g, and this value was estimated by using the copper bisethylenediamine complex method [32].

### 3.4. Scanning electron microscopy (SEM)

Scanning electron microscopy (SEM) images of the phyllosilicate samples were taken in order to verify the presence of macropores in the structure of the surfaces of matrices, since it is not possible at the magnification used in these experiments to verify micro- and mesopores structures. In the micrographs presented in Fig. 4a–d are observed the foliated structures to unmodified and modified phyllosilicates, with some fissures and holes, which indicate the presence of macroporous structure. These should contribute a little bit to the diffusion of the metallic cations to the phyllosilicate adsorbent surfaces. The number of macroporous structure is confirmed by the high specific surface areas of the modified phyllosilicates (see Table 1). As the adsorbent materials present many number of macroporous structure, it adsorbs high amount of nitrogen, which leads to a high BET surface area [17]. Therefore the major contribution of the radionuclides uptake can be attributed to micro- and mesoporous structures.

### 3.5. Effect of pH

Changes in pH of the medium are one of the most important factors affecting the concentration and actinide recovery procedure, which is related to the formation of soluble metal complexes and subsequently their stabilities in aqueous solution [5,29]. The  $\text{Th}^{4+}$ ,  $\text{UO}_2^{2+}$  and  $\text{Eu}^{3+}$  ions were examined within a range of pH 1.0–5.0. The pH of aqueous solution, which increased almost linearly pH 4.0, is an important controlling parameter in the adsorption process. Both the extent of adsorption and amount adsorbed ( $N_f^{\text{max}}$ ) showed positive charges. The influence of the pH on the concentration adsorbed for M, K, M-APPMA, and K-APPMA is shown in Fig. 5a–d, respectively and Table 2. Results emphasize that with increase in pH of solution, the  $N_f^{\text{max}}$  adsorbed increases for all systems. It can clearly be observed that adsorption is influenced a great deal by the pH of the solution and increases when the pH of the solution increased. Therefore the efficiency of metal ion adsorption on unmodified and modified phyllosilicates can be controlled by initial pH of the solid/liquid reaction. From the corresponding data for each metal, an increase in pH was followed by an increase in adsorption, reaching the maximum capacity at pH 4.0. For higher pH values it was observed a slightly decrease of adsorption for  $\text{Th}^{4+}$ ,  $\text{UO}_2^{2+}$  and  $\text{Eu}^{3+}$ , this diminution was more remarkable. The metallic ions could be suffering hydrolysis, starting at pH higher than 5.0, which promotes a diminution of the adsorption capacity, because the diminution of the formal charge of the metallic ions. Depending on the pH metal ions may form complexes with  $\text{OH}^-$ , for example,  $\text{M}(\text{OH})_n$ ,  $\text{M}(\text{OH})_{-n+1}^-$ ,  $\text{M}(\text{OH})_{-n+2}^{2-}$ , at higher pHs and as results, metal hydroxyl species may participate in the adsorption process

**Table 2**  
Thermodynamic data for radionuclides adsorption onto original and modified clay samples using clay 1.0 g dm<sup>-3</sup>, pH 4.0, time 360 min and temperature of 298 ± 1 K.

Metal	$N_f^{\text{max}}$ (mmol g <sup>-1</sup> )	pH 4.0	$N_f^{\text{max}}$ (mmol g <sup>-1</sup> )	pH	1.0	2.0	3.0	4.0–5.0	$N_s$ (mmol g <sup>-1</sup> )	$-\Delta_{\text{int}}h^\circ$ (J g <sup>-1</sup> )	$-\Delta_{\text{int}}G^\circ$ (kJ mol <sup>-1</sup> )	$n$	$K_S \times 10^{-3}$	$-\Delta_{\text{int}}C^\circ$ (kJ mol <sup>-1</sup> )	$\Delta_{\text{int}}S^\circ$ (J K <sup>-1</sup> mol <sup>-1</sup> )
K	$\text{Th}^{4+}$	1.33 ± 0.11	0.39 ± 0.01	0.48 ± 0.01	0.53 ± 0.02	1.33–1.28	1.60 ± 0.11	11.68 ± 0.12	1.60 ± 0.11	750 ± 0.10	20.9 ± 0.1	0.72	4.6 ± 0.1	20.9 ± 0.1	45 ± 1
	$\text{UO}_2^{2+}$	1.56 ± 0.13	0.45 ± 0.03	0.55 ± 0.02	0.69 ± 0.01	1.57–1.53	2.05 ± 0.11	14.78 ± 0.12	2.05 ± 0.11	721 ± 0.10	21.9 ± 0.1	0.85	7.0 ± 0.1	21.9 ± 0.1	49 ± 1
	$\text{Eu}^{3+}$	1.66 ± 0.11	0.48 ± 0.01	0.59 ± 0.01	0.93 ± 0.01	1.66–1.60	2.41 ± 0.12	17.16 ± 0.12	2.41 ± 0.12	712 ± 0.10	22.9 ± 0.1	0.93	8.4 ± 0.1	22.9 ± 0.1	52 ± 2
K-APPMA	$\text{Th}^{4+}$	6.48 ± 0.14	3.71 ± 0.01	4.71 ± 0.01	5.32 ± 0.01	6.51–6.46	7.45 ± 0.09	56.62 ± 0.12	7.45 ± 0.09	7.60 ± 0.10	21.9 ± 0.1	0.72	6.7 ± 0.1	21.9 ± 0.1	48 ± 1
	$\text{UO}_2^{2+}$	8.88 ± 0.11	4.53 ± 0.01	5.49 ± 0.02	6.75 ± 0.02	8.89–8.83	9.08 ± 0.09	66.74 ± 0.13	9.08 ± 0.09	7.35 ± 0.10	22.3 ± 0.1	0.87	8.1 ± 0.2	22.3 ± 0.1	50 ± 1
	$\text{Eu}^{3+}$	12.01 ± 0.13	4.14 ± 0.01	5.90 ± 0.05	9.19 ± 0.01	11.98–12.00	12.09 ± 0.09	88.02 ± 0.13	12.09 ± 0.09	7.28 ± 0.10	22.9 ± 0.1	0.95	10.4 ± 0.2	22.9 ± 0.1	53 ± 2
M	$\text{Th}^{4+}$	1.55 ± 0.11	0.40 ± 0.02	0.45 ± 0.04	0.76 ± 0.01	1.55–1.50	1.96 ± 0.10	8.33 ± 0.12	1.96 ± 0.10	4.25 ± 0.01	22.3 ± 0.1	0.74	8.2 ± 0.1	22.3 ± 0.1	60 ± 2
	$\text{UO}_2^{2+}$	1.66 ± 0.01	0.46 ± 0.01	0.58 ± 0.03	0.89 ± 0.01	1.66–1.57	2.61 ± 0.12	13.39 ± 0.12	2.61 ± 0.12	5.13 ± 0.11	23.3 ± 0.1	0.85	12.2 ± 0.1	23.3 ± 0.1	61 ± 2
	$\text{Eu}^{3+}$	1.86 ± 0.11	0.57 ± 0.03	0.77 ± 0.01	0.96 ± 0.04	1.87–1.81	2.93 ± 0.11	16.42 ± 0.12	2.93 ± 0.11	5.51 ± 0.10	24.2 ± 0.1	0.93	17.2 ± 0.1	24.2 ± 0.1	61 ± 2
M-APPMA	$\text{Th}^{4+}$	7.47 ± 0.11	3.75 ± 0.02	4.30 ± 0.03	5.63 ± 0.01	7.48–7.42	8.02 ± 0.09	34.89 ± 0.11	8.02 ± 0.09	4.35 ± 0.11	22.6 ± 0.1	0.77	9.3 ± 0.1	22.6 ± 0.1	61 ± 1
	$\text{UO}_2^{2+}$	9.83 ± 0.12	4.53 ± 0.02	5.77 ± 0.01	6.96 ± 0.01	9.88–9.78	10.63 ± 0.20	56.76 ± 0.11	10.63 ± 0.20	5.34 ± 0.11	23.7 ± 0.1	0.89	15.5 ± 0.1	23.7 ± 0.1	61 ± 1
	$\text{Eu}^{3+}$	12.93 ± 0.11	5.66 ± 0.01	7.16 ± 0.01	9.45 ± 0.02	13.04–12.94	14.65 ± 0.20	84.09 ± 0.11	14.65 ± 0.20	5.74 ± 0.11	24.3 ± 0.1	0.97	19.2 ± 0.1	24.3 ± 0.1	62 ± 1

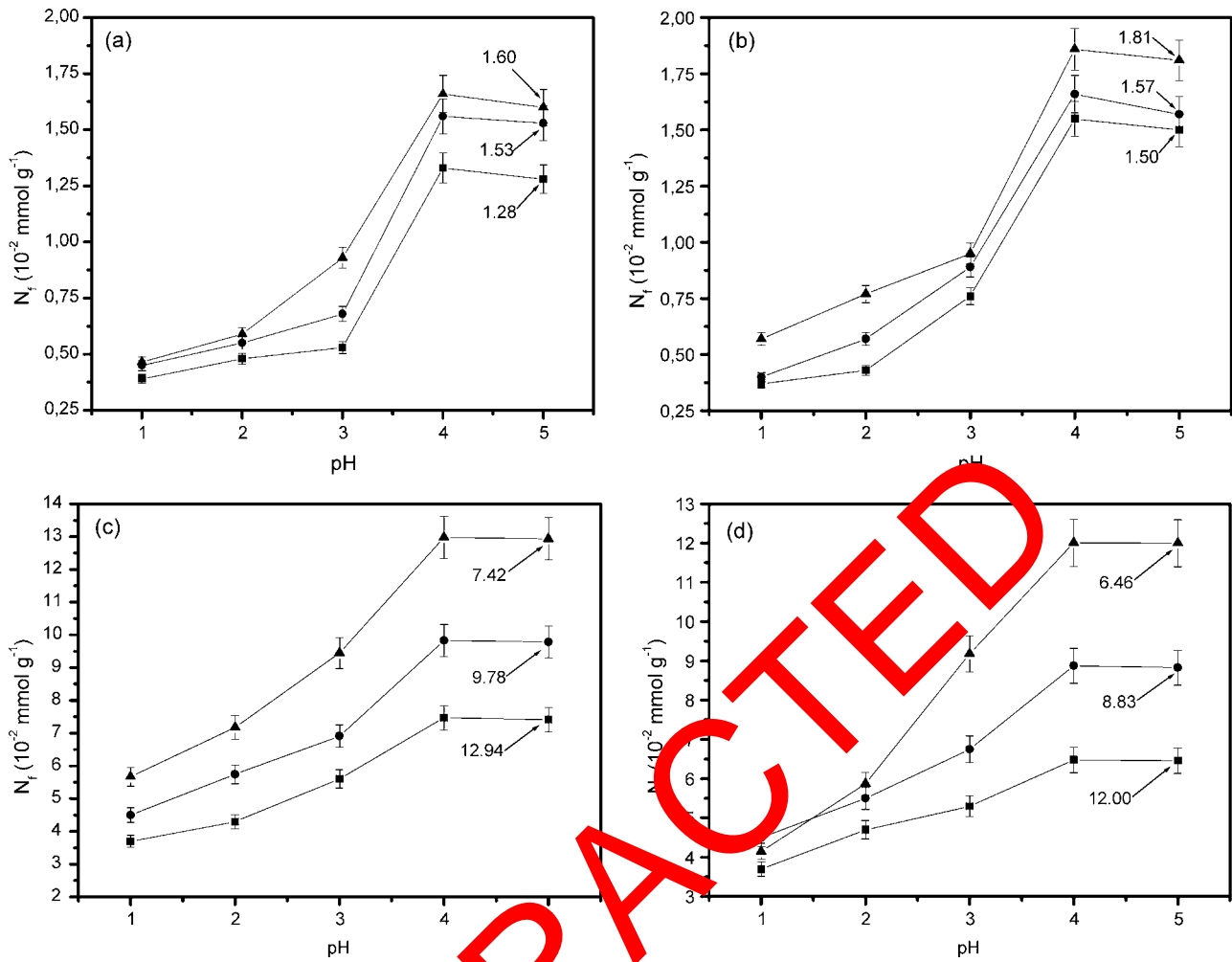
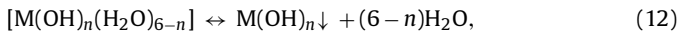
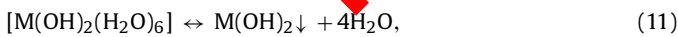
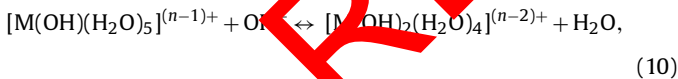
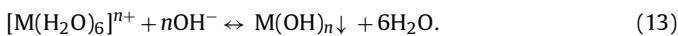


**Fig. 5.** Effect of pH on the adsorption of radionuclides onto clay samples (a), K(b), M-APPMA (c) and K-APPMA (d) (clay  $1.0 \text{ g dm}^{-3}$ , time 360 min and controlled temperature in  $298 \pm 1 \text{ K}$ ) ( $\text{Th}^{4+}$  ■,  $\text{UO}_2^{2+}$  ● and  $\text{Eu}^{3+}$  ▲).

and precipitate onto adsorbent surface. The following equations for metal ions as a function of pH have been expected (Eq. (9)–(13)) [33,34].



where  $\text{M} = \text{Th}(\text{IV})$ ,  $\text{U}(\text{VI})$  and  $\text{Eu}(\text{III})$ . Precipitation of  $\text{M}(\text{OH})_2$  on the solid surface;



In addition, as pH is increased there is a decrease of positive surface charge, which results in lower coulombic repulsion of the adsorbing metal ions. Consequently the number of moles of metal ions removal may decrease at low pH [8].

### 3.6. Effect of metal concentration variation

The clay samples have been used to evaluate the maximum adsorption capacity for uptaking metal ions, such as  $\text{Th}^{4+}$ ,  $\text{UO}_2^{2+}$  and  $\text{Eu}^{3+}$ , from aqueous solutions. In fact, these cations act as acidic

Lewis centers that interact with the basic Lewis center attached to the pendant molecules covalently bonded to the modified clay surfaces [14,25]. Such processes occurring at the solid/liquid interface give the isotherms that demonstrate the saturation of the original and modified clay samples with a definite number of moles of metallic cations, as clearly shown in Fig. 6a–d with the highest pronounced adsorption for europium and the Sips equation values were obtained with non-linear regression for all systems [35–41]. The maximum adsorption capacity,  $N_f^{\text{max}}$ , for each metal halide on silicate matrices is listed in Table 2, which presented the values 7.47, 9.83 and 12.93  $\text{mmol g}^{-1}$  for  $\text{Th}^{4+}$ ,  $\text{UO}_2^{2+}$  and  $\text{Eu}^{3+}$ , respectively (M-APPMA) and 6.48, 8.88 and 12.01  $\text{mmol g}^{-1}$  for  $\text{Th}^{4+}$ ,  $\text{UO}_2^{2+}$  and  $\text{Eu}^{3+}$ , respectively (K-APPMA). The applicability of these kinds of porous materials depends on a series of properties, on the degree of molecules immobilized, mainly when the adsorption is considered. In addition, the variation in adsorption capacities of these metal ions probably arises due to differences in their sizes, degree of hydration and binding constants with the chelating matrix.

### 3.7. Thermodynamic study

In environmental engineering practice, both energy and entropy factors must be considered in order to determine which process will occur spontaneously. The adsorption processes were also calorimetrically monitored by titration process. From these values, the thermal effect related to cation–basic center interactions on the

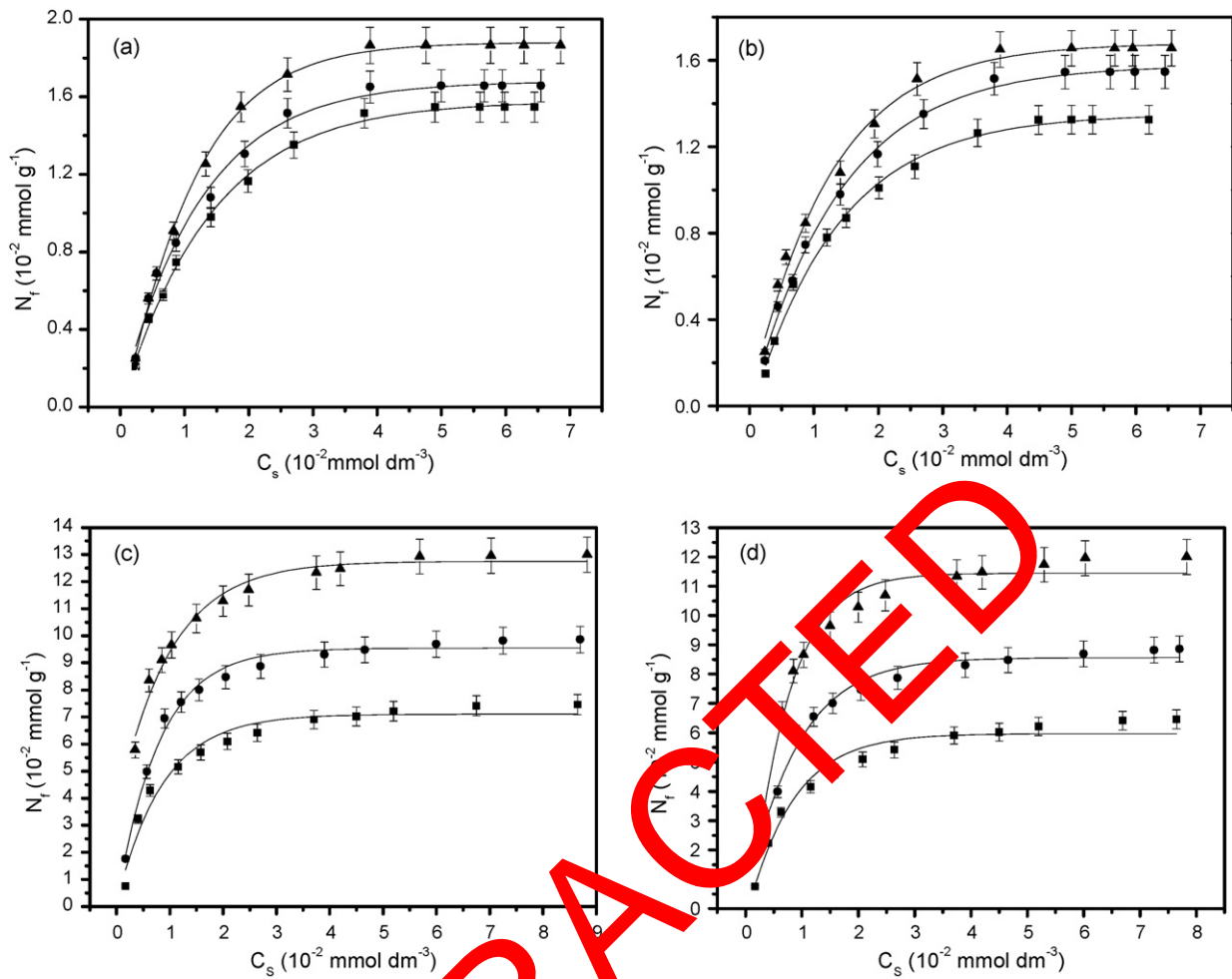


**Fig. 6.** Metals ions adsorption onto clay samples: M (a), K (b) M-APPMA (c) and K-APPMA (d) ( $Th^{4+}$  ■,  $UO_2^{2+}$  ● and  $Eu^{3+}$  ▲) (clay  $1.0$   $g$   $dm^{-3}$ , pH 4.0, time 360 min and controlled temperature in  $298 \pm 1$  K).

modified surfaces is obtained. The steps of calorimetric titrations of unmodified and modified matrices with metal ions solutions are shown in Fig. 7a and b. The respective curves for europium obtained with non-linear regression [42], given in Fig. 8a and b shows, as an example, one of the titration thermograms obtained when M-APPMA adsorbs the europium cation. It shows that, under the conditions applied, equilibrium is attained rapidly. Complete sets of thermodynamic data for each system studied are listed in Table 2. As

observed, cation/basic center interactions for all systems are spontaneous in nature as reflected their negative enthalpic values. The series of exothermic enthalpic data did not permit distinguishing a preference of any particular cation to bond with the available basic centers attached to the pendant groups covalently bonded to the inorganic backbone. However, the positive entropic values for all interactions that contribute to the favorable interactive process are associated with solvent molecules displacement, initially

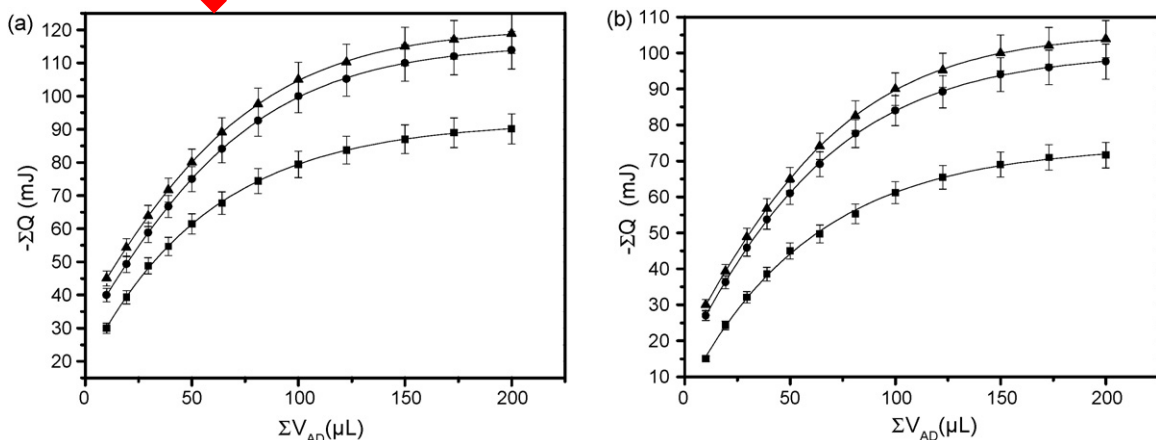


**Fig. 7.** The resulting thermal effects of the adsorption isotherms for the radionuclides: ( $Th^{4+}$  ■,  $UO_2^{2+}$  ● and  $Eu^{3+}$  ▲) M-APPMA (a) and K-APPMA (b).



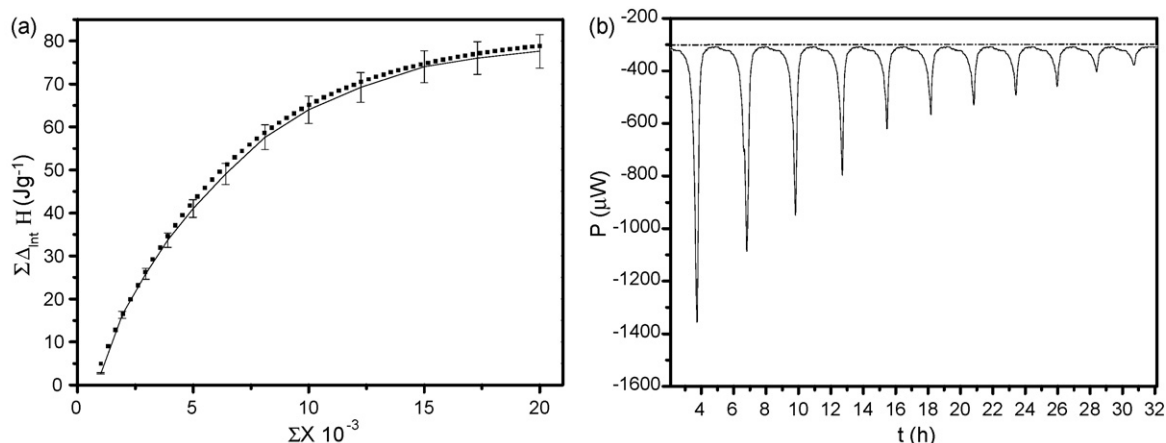


**Fig. 8.** An example of curve of thermal effect and calculated curve obtained by non-linear regression (adsorption of  $\text{Eu}^{3+}$  into M-APPMA) (a) and variation of the thermal effect versus time upon microcalorimetric titration of M-APPMA suspended in water with  $20.0 \text{ cm}^{-3}$  of  $\text{Eu}^{3+}$  at  $298 \pm 1 \text{ K}$  (b).

bonded to the modified clays, which is reinforced by desolvation of the cations before interacting with the basic centers. In such interactive processes the increase in free molecules in the reaction medium gives positive entropy, thus demonstrating a favorable set of thermodynamic data for this kind of system [14,21,43].

#### 4. Conclusions

In conclusion, the metals adsorption study onto the modified montmorillonite and kanemite structures demonstrated that the inorganic–organic hybrid materials can act as chelating agents in pollutant metal ion removal from aqueous solution. Based on the capacity of adsorption of the natural, synthetic and modified clays to interact metallic ions, the following results were obtained  $6.48$ ,  $8.88$  and  $12.01 \text{ mmol g}^{-1}$  for  $\text{Eu}(\text{III})$ ,  $\text{U}(\text{VI})$  and  $\text{Th}(\text{IV})$ , respectively. Reflecting a maximum adsorption order of  $\text{Eu}(\text{III}) > \text{U}(\text{VI}) > \text{Th}(\text{IV})$ . The maximum adsorption capacities vary with pH values, being higher at pH 4.0, which was experimentally fixed at  $298 \pm 1 \text{ K}$  for all adsorptions. The quantitative of metal/reactant center interactions for original and chemically modified clays were followed through calorimetric titration at the solid/liquid interface to give favorable sets of data, such as exothermic enthalpy, negative free Gibbs energy, and positive entropic values. These thermodynamic data suggest the application of this series of synthetic, natural and modified layer materials to improve the environment as cation extraction agents. The structural features of the new synthesized materials with long designed chain suggested that it could suitably be modified further by several other synthetic approaches, to yield higher stage pendant chains, for a wide variety of chemical applications.

#### Acknowledgements

The authors are indebted to CNPq for fellowships and FAPESP for financial support.

#### References

- [1] F.A. Pavan, I.S. Lima, E.C. Lima, C. Airoldi, Y. Gushiken, Use of pokan mandarin peels as biosorbent for toxic metals uptake from aqueous solution, *J. Hazard. Mater.* 137 (2006) 527–533.
- [2] T. Kanno, H. Mimura, Ion Exchange Properties of Zeolites and their Application to Processing of High Level Liquid Waster, IAEA-TEC-DOC-337, International Atomic Energy Agency, Vienna, 1985, p. 237.
- [3] D.L. Guerra, C. Airoldi, R.R. Viana, Performance of modified montmorillonite clay in mercury adsorption process and thermodynamic studies, *Inorg. Chem. Commun.* 11 (2008) 20–24.
- [4] D.L. Guerra, V.P. Lemos, C. Airoldi, R.S. Angélica, Influence of the acid activation of pillared smectites from Amazon (Brazil) in adsorption process with butylamine, *Polyhedron* 25 (2006) 2880–2890.
- [5] D.L. Guerra, C. Airoldi, V.P. Lemos, R.S. Angélica, Adsorptive, thermodynamic and kinetic performances of Al/Ti and Al/Zr pillared clays from the Brazilian Amazon region for toxic cation removal, *J. Hazard. Mater.* 155 (2008) 230–242.
- [6] M.H. Yu, *Environmental Toxicology—Biological and Health Effects of Pollutants*, 2nd ed., CRC Press, Boca Raton, 2005.
- [7] OECD Nuclear Energy Agency, *Ecological Disposal of Radioactive Waster: Review and Developments of the Last Decade*, Paris, 1999.
- [8] I. Villacusa, J. Martínez, N. Miralles, Heavy metal uptake from aqueous solution by cork and mimbe bark wastes, *J. Chem. Technol. Biotechnol.* 75 (2000) 89–96.
- [9] T. Shahwan, H.N. Erten, Characterization of  $\text{Sr}^{2+}$  uptake on natural minerals of kaolinite and magnetite using XRPD, SEM/EDS, and DRIFT, *Radiochim. Acta* 93 (2005) 225–232.
- [10] S. Babel, T. Kurniawan, Low-cost adsorbents for heavy metals uptake from contaminated water: a review, *J. Hazard. Mater.* 97 (2003) 219–243.
- [11] R. Day, C. Airoldi, Designed pendant chain covalently to silica gel for cation removal, *J. Hazard. Mater.* 156 (2008) 95–101.
- [12] D. Mohan, K.P. Singh, V.K. Singh, Removal of hexavalent chromium from aqueous solution using low-cost activated carbons derived from agriculture waste materials and activated carbon fabric cloth, *Ind. Eng. Chem. Res.* 44 (2005) 1027–1042.
- [13] R.A. Jacques, R. Bernardi, M. Caovila, E.C. Lima, F.A. Pavan, J.C.P. Vagheti, C. Airoldi, Removal of  $\text{Cu}(\text{II})$ ,  $\text{Fe}(\text{II})$  and  $\text{Cr}(\text{VI})$  from aqueous solution by aniline grafted silica gel, *Sep. Sci. Technol.* 42 (2007) 591–609.
- [14] J.A.A. Sales, C. Airoldi, Calorimetric investigation of metal ion adsorption on 3-glycidioxypropyltrimethylsiloxane + propane-1,3-diamine immobilized on silica gel, *Thermochim. Acta* 427 (2005) 77–83.
- [15] D.L. Guerra, A.A. Pinto, C. Airoldi, R.R. Viana, Adsorption of uranyl (II) into modified lamellar Na-kanemite, *Inorg. Chem. Commun.* 3 (2008) 23–26.
- [16] L.J. Twyman, A.S.H. King, J. Burnet, I.K. Martin, Synthesis of aromatic hyper-branched PAMAN polymers, *Tetrahedron Lett.* 45 (2004) 433–435.
- [17] S. Brunauer, P.H. Emmett, E.E. Teller, The adsorption of gas in multimolecular layer, *J. Am. Chem. Soc.* 60 (1938) 309–319.
- [18] E.P. Barret, L.G. Joyner, P.P. Halenda, The determination of pore volume and area distribution in porous substances. I. Computation from nitrogen isotherms, *J. Am. Chem. Soc.* 73 (1951) 373–380.
- [19] J.M. Thomas, Solid state NMR and the characterization of zeolites: its genesis, some early errors and final triumph, *Microporous Mesoporous Mater.* 114 (2007) 5–9.
- [20] R. Sips, On the structure of a catalyst surface, *J. Chem. Phys.* 16 (1948) 490–495.
- [21] A.M. Lazarin, C. Airoldi, Thermochemistry of intercalation of n-alkylmonoamines into lamellar hydrated barium phenylarsonate, *Thermochim. Acta* 454 (2007) 43–49.
- [22] T.R. Macedo, G.C. Petrucelli, C. Airoldi, Silicic acid magadiite guest molecules and features related to the thermodynamics of intercalation, *Clay Clay Miner.* 55 (2007) 151–159.
- [23] A.R. Cestari, E.F.S. Vieira, G.S. Vieira, L.P. da Costa, A.M.G. Tavares, W. Loh, C. Airoldi, The removal of reactive dyes from aqueous solutions using chemically modified mesoporous silica in the presence of anionic surfactant—the temperature dependence and a thermodynamic multivariate analysis, *J. Hazard. Mater.* 161 (2009) 307–316.
- [24] V.S.O. Ruiz, C. Airoldi, Thermochemical data for n-alkylmonoamine intercalation into crystalline lamellar zirconium phenylphosphonate, *Thermochim. Acta* 420 (2004) 73–78.
- [25] P. Sharma, R. Tomar, Synthesis and application of an analogue of mesolite for removal of uranium(VI), thorium(IV), and europium(III) from aqueous waste, *Microporous Mesoporous Mater.* 116 (2008) 641–652.
- [26] N.L. Dias Filho, Adsorption of copper(II) and cobalt(II) complexes on a silica gel surface chemically modified with 3-amino-1,2,4-triazole, *Colloids Surf. A* 144 (1998) 219–227.

- [27] A.G.S. Prado, C. Airoidi, Different neutral surfactant template extraction routes for synthetic hexagonal mesoporous silicas, *J. Mater. Chem.* 12 (2002) 3823–3826.
- [28] K. Albert, E. Bayer, Characterization of bonded phases by solid-state NMR spectroscopy, *J. Chromatogr. Sci.* 544 (1991) 345–370.
- [29] M. Hughes, P. Miranda, D. Nielsen, E. Rosenberg, R. Gobetto, A. Viale, S. Burton, Silica polyamine composite: new supramolecular materials for cation and anion recovery and remediation, *Macromol. Symp.* 235 (2006) 161–178.
- [30] D.P. Quintanilla, I. Del Hierro, M. Fajardo, I. Serra, Preparation, characterization, and Zn<sup>2+</sup> adsorption behavior of chemically modified MCM-41 with 5-mercapto-1-methyltetrazole, *J. Colloid Interface Sci.* 313 (2007) 551–562.
- [31] D.P. Quintanilla, I. Del Hierro, M. Fajardo, I. Serra, 2-Mercaptothiazoline modified mesoporous silica for mercury removal from aqueous media, *J. Hazard. Mater.* 134 (2006) 245–256.
- [32] K.G. Bhattacharyya, S.S. Gupta, Pb(II) uptake by kaolinite and montmorillonite in aqueous medium: influence of acid activation of the clays, *Colloids Surf. A* 277 (2006) 191–200.
- [33] P. Sharma, G. Singh, R. Tomar, Synthesis and characterization of an analogue of heulandite: sorption and applications for thorium(IV), europium(III), samarium(II) and iron(II) recovery from aqueous waste, *J. Colloid Interface Sci.* 332 (2009) 298–308.
- [34] J.E. Huheey, E.A. Keiter, R.L. Keiter, *Inorganic Chemistry: Principles of Structure and Reactivity*, Harper Collins, New York, 1993.
- [35] G. Sheng, J. Hu, X. Wang, Sorption properties of Th(IV) on the raw diatomite—effects of contact time, pH, ionic strength and temperature, *Appl. Radiat. Isotopes* 66 (2008) 1313–1320.
- [36] D. Leppert, Heavy metal sorption with clinoptilolite zeolite: alternatives for treating contaminated soil and water, *J. Mining Eng.* 42 (1990) 604–608.
- [37] S.H.M. Evangelista, E. De Oliveira, G.R. Castro, L.F. Zara, A.G.S. Prado, Hexagonal mesoporous silica modified with 2-mercaptothiazoline for removing mercury from water solution, *Surf. Sci.* 601 (2007) 2194–2202.
- [38] C.L. Chen, X.K. Wang, Sorption of Th(IV) to silica as a function of pH, humic/fulvic acid, ionic strength electrolyte type, *Appl. Radiat. Isotopes* 65 (2007) 155–163.
- [39] X. Tang, Z. Li, Y. Chen, Adsorption behavior of Zn(II) on calcinated Chinese loess, *J. Hazard. Mater.* 161 (2009) 824–834.
- [40] W. Xiu-Wen, M. Hong-Wen, L. Jin-Hong, J. Zhang, L. Zhi-Hong, The synthesis of mesoporous aluminosilicate using microcline for adsorption of mercury(II), *J. Colloid Interface Sci.* 315 (2007) 555–561.
- [41] B. Salih, A. Denizli, C. Kavakli, E. Pişkin, Adsorption of heavy metal ions onto dithizone-anchored poly(EGDMA-HEMA) microbeads, *Talanta* 46 (1998) 1205–1213.
- [42] D. Karadag, Y. Koc, M. Turan, M. Ozturk, A comparative study of linear and non-linear regression analysis for ammonium exchange by clinoptilolite zeolite, *J. Hazard. Mater.* 144 (2007) 432–437.
- [43] J.A.A. Sales, A.G.S. Prado, C. Airoidi, Interaction of divalent copper with two diaminealkyl hexagonal mesoporous silicas evaluated by adsorption and thermodynamic data, *Surf. Sci.* 566 (2005) 51–62.

RETRACTED